

a NASA facsimile reproduction

of

CASE FILE COPY

11/64-11106

REPRODUCTION OF THIS DOCUMENT IS UNAUTHORIZED PRACTICE AND IS PROHIBITED									
NO. 3 117231 (ACT. 1 OF 1)									
SEARCHED INDEXED SERIALIZED FILED 11/18/64									
SCIENTIFIC INSTITUTE OF TECHNOLOGY IN FACILITY									
REPRO									
OF FORM									



MICROFILMED
FROM BEST
AVAILABLE
COPY

N 64 1106
SINGOLASS
CODE 1

MONTHLY PROGRESS REPORT NO. 3

Covering period from October 1, 1963 to October 31, 1963

Contract N 33-2769

29
N 64 11106
Cleve 1
AB 36 CTC ST 5261

BRATTON CTC & SOLAR COLLECTOR
TESTING EQUIPMENT PROGRAM

Item 12. A.

1.3 PREVIOUS DATES TO THE REPORTING PERIOD

1.1 General Comments

The initial study and analytical portion of the program is nearing completion and simulation and optimization of analytical results are being made before the final two month detailed design phase.

Homogeneous sandwich materials have been shown to be a highly efficient structural concept and analysis made during this reporting period show that thermal gradients due to a continuous insulating agent will not produce excessive thermal distortions.

Optimal performance analysis approaches have been finalized for parametric concentrator evaluations, and a computer program which is available at Aerospace Corporation appears to be an excellent source for combined concentrator performance predictions.

Bowl study tasks have stopped schedule, and repeat technical directions by NASA, Lewis, to investigate the microconcentrator evanescent environment in more detail has resulted in some late modifications.

LIBRARY COPY

TECHMSON RAYONIER INC.
New Product Research
Cleve. Sub. Inc.
Project 512-004235-08

OTS PRICE

XENIX : Bill G.
MICRONT : Bill G.
CBO Department

November 12, 1963
Date

1.2 Performance Analysis

- 1.2.1 Parametric Calculations

The concentrator performance analysis has been finalized and its results in the following expression for fiber distribution on the focal plane

$$K(r, \alpha) = \frac{K(r_0 - r)}{2\pi \int_{r_0}^{r_1} \frac{1}{r'^2} dr'}$$

where the integral,

$$I(r, \alpha) = \int_{r=0}^{\infty} \int_{\alpha=0}^{\pi} e^{-\frac{r}{2f}} e^{-\frac{r^2}{2f^2}} d\alpha \frac{r^2}{2f^2} dr$$

Refer to Progress Report 10, 1 for nomenclature.

Integration of this expression has been obtained by numerical methods and the entire equation has been programmed on a digital computer. Computed results for a typical case, with and without absorption, are shown in Figures 1 and 2. This level is in terms of flux concentration which is the sum of multiple reflectivity or structure shadowing. The reflect rate and does not include reflection from the collector. The effect of absorption can best be seen in Figure 3 which is a contour plot of lines of constant flux concentration.

In addition to this modified Rivers approach, a theoretical analysis of solar radiation which was developed by Dr. G. I. Schowalter was also investigated during this reporting period. An analytical model and computer solution was developed through Aerospace Corporation and is now available for use. Dr. Schowalter was consulted to determine the applicability of this analysis to the Brayton model for study requirements. Computer results presented to the Brayton model for study requirements were compared to the 30 foot diameter collector. Results of interest are plotted in Figure 4 and the results of black body radiation loss from an optimum aperture based on the perfectly reflected case. Additional results which are presently available are being obtained. The solution computed from the modified Rivers approach (Figure 1) is also shown as a comparison data point in Figure 4.

The optimum aperture sizes shown in Figure 4 are based on black body radiation from the aperture at zero absorber/dissipation conditions. The 30 foot radius of curvature of the collector is assumed which has no impact on options will vary with the actual formulation conditions which can affect the black body) and with absorber/dissipation. Effects of these parameters will be shown in Figure 5. It is seen that a band of performance to possible viable the orientation tolerances for while specific sizes of collector geometry. Other cases are being calculated to investigate the full range of performance performance.

Due to time and budget considerations, it is anticipated that the Aerospace computer program will be utilized to predict only the final collector performance. Parametric comparisons will continue using the modified Rivers approach.

Siem Aerospace is also developing an associated computer solution of cavity receiver performance. It is especially desirable to compare the final collector-receiver performance utilizing this technology.

1.2.2 Surface Error Extractions

Surface error inspections of a five foot diameter stretch formed concentrator have been completed. This concentrator is typical of the stretch formed glass or sector type construction which is contemplated for the Brayton collector. A point source of light in combination with a grid and eyepiece was used as the inspection approach. Inspections were performed at various stages of fabrication to identify sources of error and to add to accuracy extrapolation to a 20 and 30 foot diameter collector. Inspection data are now being reduced and the following types of deviations have been identified as being applicable to the Brayton collector:

stretch replication errors
Shell assembly spring-back errors
Support ring induced errors
Total combined errors

The magnitude and distribution of these deviations will be combined with probable tooling errors and any other sources of error which might be characteristic of the Brayton collector size and design, to retain a realistic prediction of surface quality for use in collector performance calculations.

1.3 Thermal Analysis

The calculation of view factors at various collector locations for earth thermal radiation was started. The average view factor for frost and thermal radiation was started. The average view factor at the rim were obtained, both sides of the 30 foot diameter concentrator at the rim were obtained. The view factor of an incremental area on the concentrator is a function of the orbital position, surface slope, orbital altitude and shadowing effect of the concentrator. To reduce the complexity, the shadowing effects of the radiator was neglected.

The combined effect of orbital positions, surface plane and attitude in the angle between the line from center to collector and the normal to the surface. Depending upon the position of the collector and the normal by the remainder of the shadowed area under consideration will vary for certain portions of the orbit.

Figures 7 and 8 show plots of the correction factor and the ratio of the corrected view factors of other circular average view factor for the front-reflective location at a given orbital position as a non-rotating curve. The total average view factor and temperature distribution at the given radius of the concentrator is then calculated for the given radius of the collector. Figure 9 shows the calculations for the mid-radius position of the collector.

1.4 Structural Analysis

1.4.1 Distortion Results From a Temperature Increase of the Shell

Suppose the spherical cap of thickness t_1 has a temperature increase ΔT with respect to the center, consider a thin shell of thickness t_1 with a constant thermal expansion coefficient α . Then the stress in the shell is

$$\frac{\alpha(\Delta T + T_1)}{2}$$

For the unstrained shell, stresses are everywhere zero due to axial symmetry. The two thermal stress due to this change in temperature increase in front diameter collector that were applied to the boundary, that is, stresses free requires that a moment be applied at the boundary. This is illustrated in figure 10. Importantly, should

Figure 10
TAPCO - A torus that is attached to the shell will offer restraint to the ring relative to the rest of the shell. While the magnitude of this distortion will be small as well as only near the edge, it is known that the geometry of the shell is specific design, it is known that the geometry has not yet been determined and for this will be discussed in section 1.4.2.

1.4.2 Temperature Gradient Across the Thickness of the Section

Distortion due to temperature gradients across the thickness of the section are often taken equal to those of the section cap will behave the same if we consider a uniform flat plate.

A more realistic approach would be to consider the thickness of the shell there in the complete shell. If we impose at the boundary the boundary the stresses that exist there compared to the center, consider a hollow sphere for temperature variation in the complete shell, in particular at the same thickness to middle point, namely,

$$\sigma_{rr} = -E\Delta T$$

$$(1)$$

The complete sphere for any temperature distribution due to an average temperature free. It may have grown slightly in respect to the center will be distortion free. The symmetry of the profile provides above sum reference levels. For the partial shell to remain distortion or rotation of one

applied at the boundary, that is, stresses free requires that a moment be applied at the boundary. This is illustrated in figure 10. Importantly, should not be relieved there. This is a requirement that a moment be applied at the boundary. This is illustrated in figure 10. Importantly, should

TAPCO "Division of
Thompson Ramo Wooldridge Inc."

Page -7-
Thompson Ramo Wooldridge Inc.

the moment provided by the ring differ from that required, the difference will only locally distort the shell.

It is concluded that a partial shell will remain almost entirely free of distortion due to a temperature gradient through the thickness. It looks just like an unrestrained stress-free flat plate that deforms due to a linear AT, but rather like a built-in plate that has stresses built in free of distortions.

1.4.3 Shell Distortion Resulting From Ring Forces

Shell rotation as a function of arc length for a fixed edge moment has been determined. Figure 11 indicates the results for the 30 foot concentrator of .050 inch thickness. As an approximation, the arc length is affected for a distance

$$\theta = 1.42 \sqrt{\frac{R}{h}}$$

where R = radius of curvature of equivalent spherical shell

h = shell thickness

For the 30 foot concentrator, the arc length affected for $h = .050$ in. is about 5.3 in.; for $h = .50$, $\theta = 16.9$ in.

1.4.4 Further Comment on Shell Distortion

In "Ring Theory" as reported in the Proceedings of the Fourth Midwest Conf. on Solid Mechanics the size of the buckling displacements are indicated by the diagram in

$$\theta = 7.0 \sqrt{\frac{h}{R}} \text{ radians}$$

For a .050 inch thick 30 foot dia. shell, θ is 4.4 degrees; are length subdivided is about 31 inches. The question - based on an axis symmetrical buckle and large deflection theory - indicates that little is gained if a

thin shell is supported at only a limited number of points. Local conditions can only a small portion of the sphere are important.

1.4.5 Local Instability of Honeycomb Sandwich Construction

Overall instability of the shell was discussed in last month's Progress Report. Honeycomb core orientation requires, in addition, that checks be made to insure against local failure.

The form is monocell buckling, or buckling of individual cells within the honeycomb core. Results are indicated in Figure 12. To insure a distortion free surface, one would not want to use 3/8 inch cells with a facing thickness less than .008 inch nor 1/4 inch cells with a facing thickness less than .006 inch.

Wrinkling or distortion over a series of cells may occur if the core does not have sufficient ability to stabilize the faces. The limiting criterion indicates that one should not use thick (.012 inch) facing with thin (.003 inch) core material. Thick changes and .002 inch core material are safe.

1.4.6 Structural Specimens & Tests

Materials have been ordered for the fabrication of small specimens to aid in structural concept evaluations. Specimens of various face thickness and environments on the specimen while mounted in a Prof. border variance investigation instrument. These variances measure cell warps and any thermal distortion within the cell.

A specimen holder is being designed which will apply anticipated thermal environments on the specimen while mounted in a Prof. border variance investigation instrument. These variances measure cell warps and any thermal efficient weight and optical quality structural design.

2.0 PROBLEMS AND CORRECTIVE ACTION

Certain tank areas have collapsed and are approximately two weeks behind schedule. Also, the recent technical direction to support erosion investigations have resulted in the schedule modifications shown in the attached task schedule. Since certain key

Page 4
TAPCO, a division of
Thomson Manufacturing Inc.

personnel must be used in the preparation of specimens and the associated
microstructure problem investigation, the finalized temperature map calculations
will be delayed.

3.0 WORK TO BE PERFORMED DURING THE NEXT MONTH

As above in the attached task schedule, all effort will be directed toward
optimizing and finalizing the structural design documents and optimal geometry an
that detailed report and design can proceed in December.
Microstructure analysis experiment specimens will be prepared and reference reflect-
ivity measurements obtained.

TASK SCHEMATIC

No. 1000 of
1947

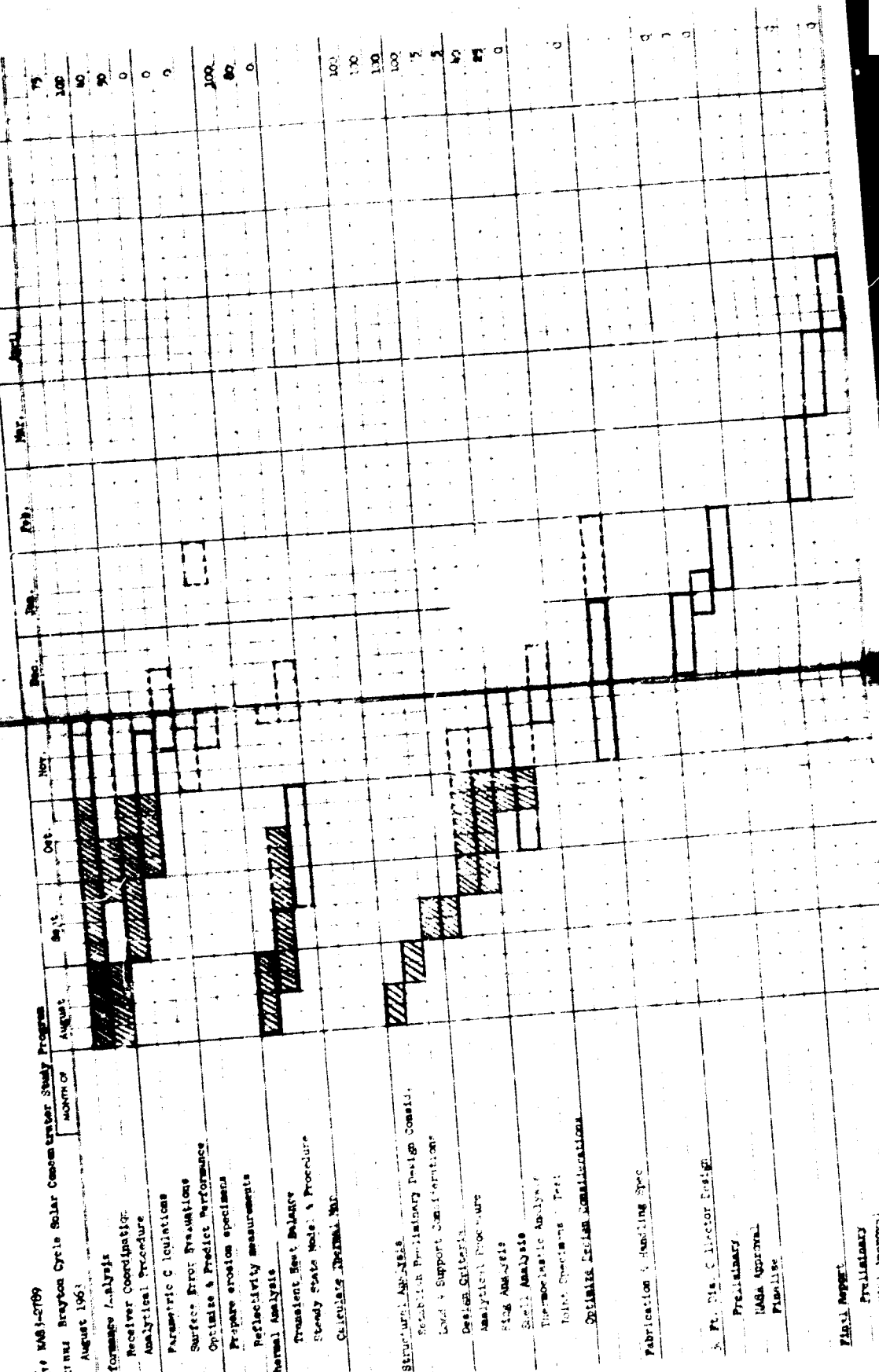
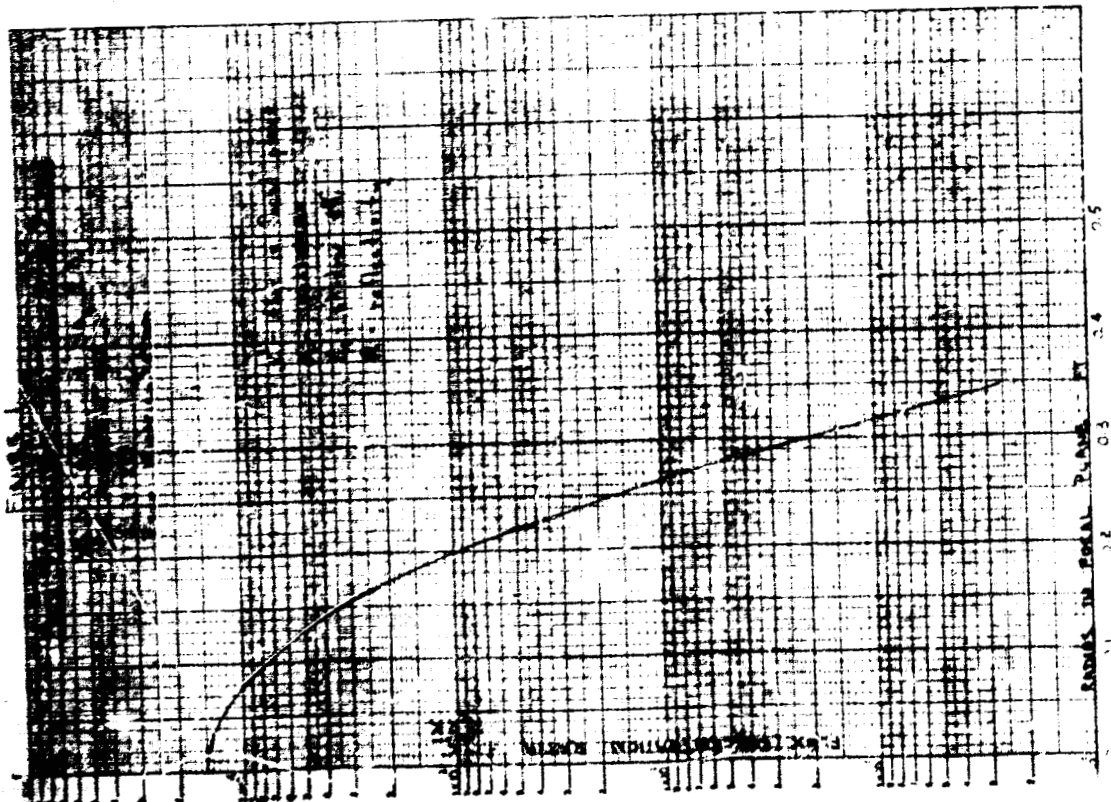
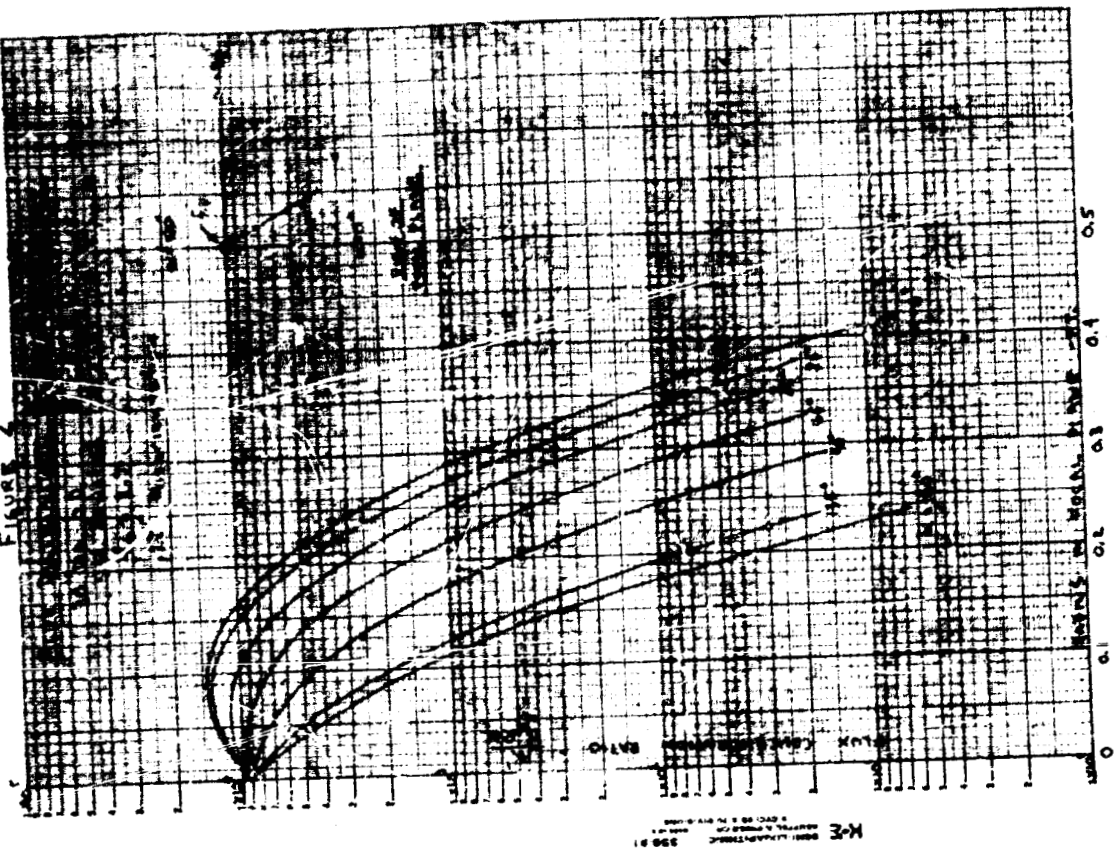


FIGURE 2



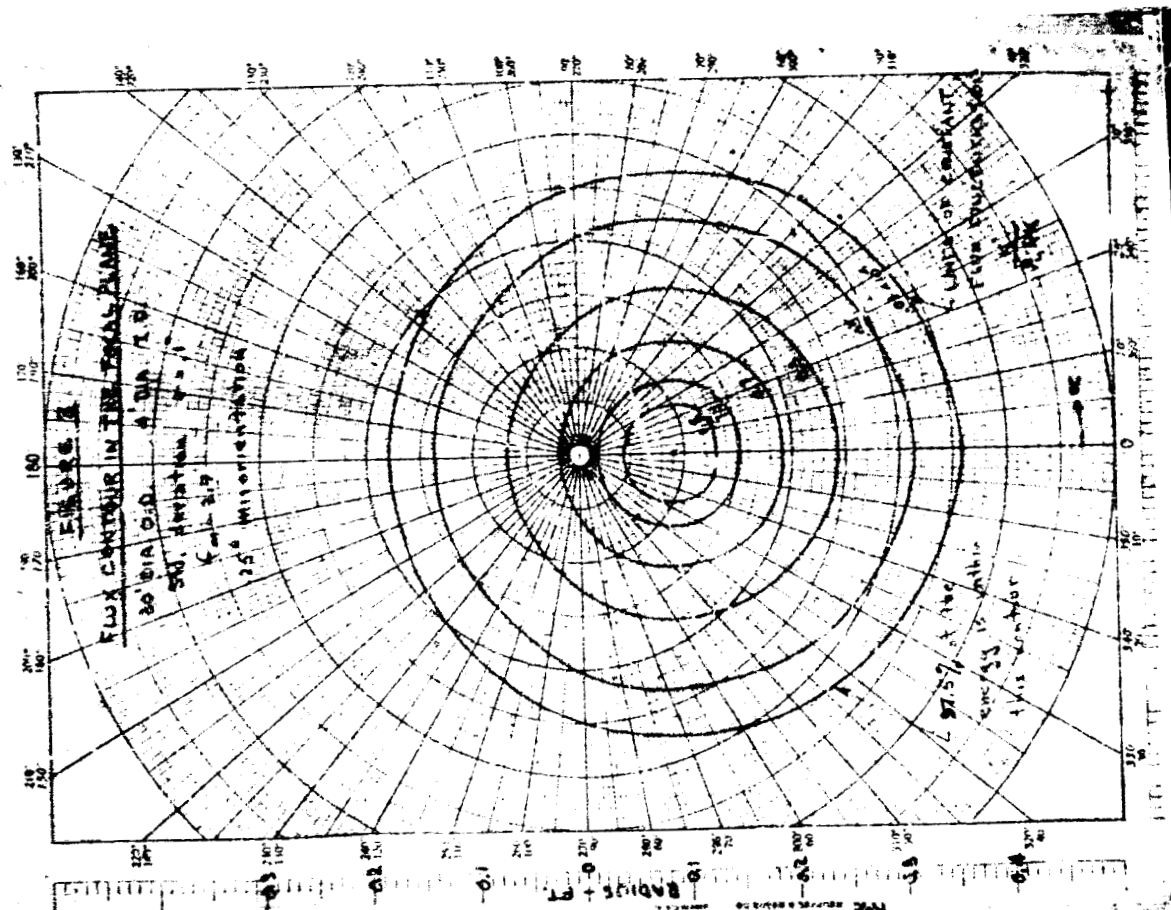


Figure 1

30 ft. dia. 6.0
black body radiation at 1000°
heat absorption

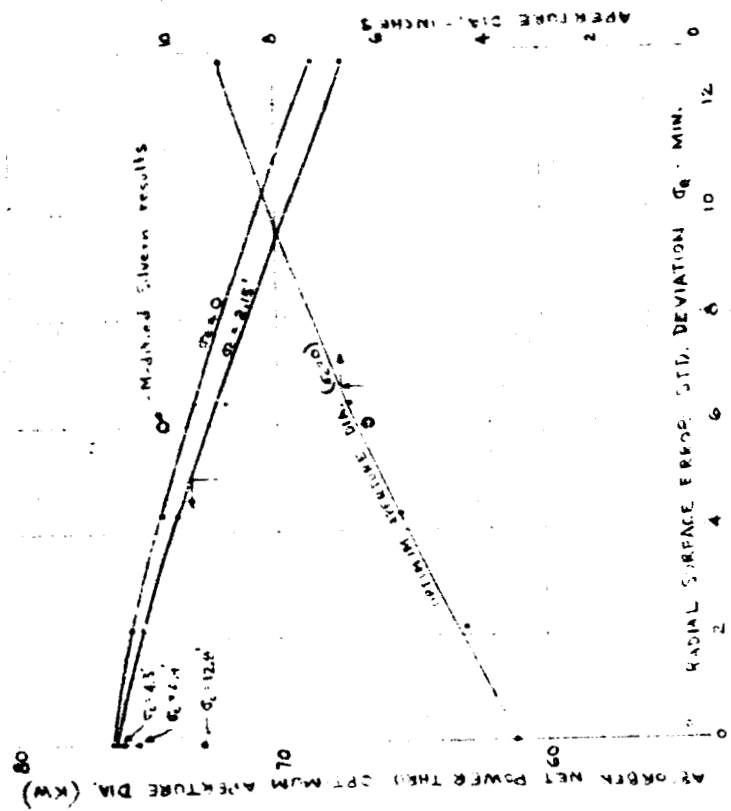
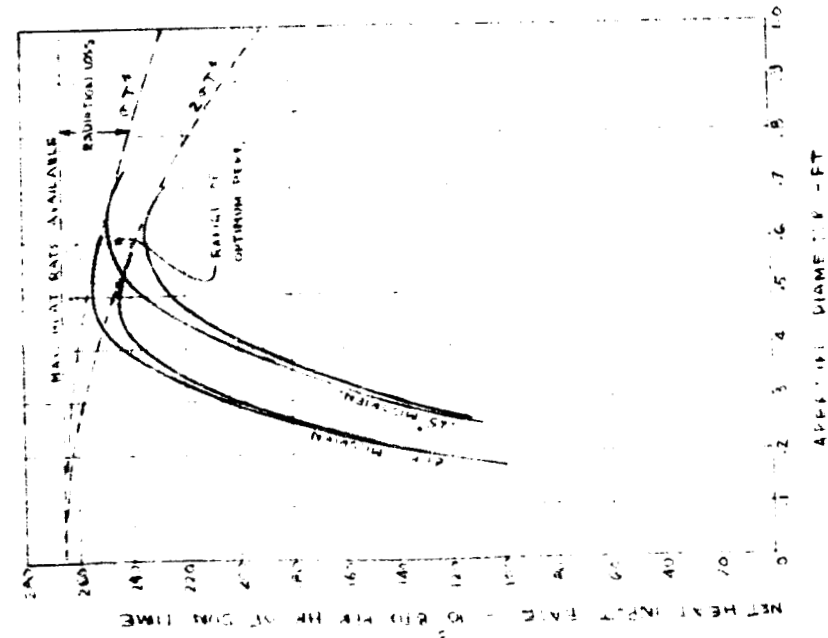
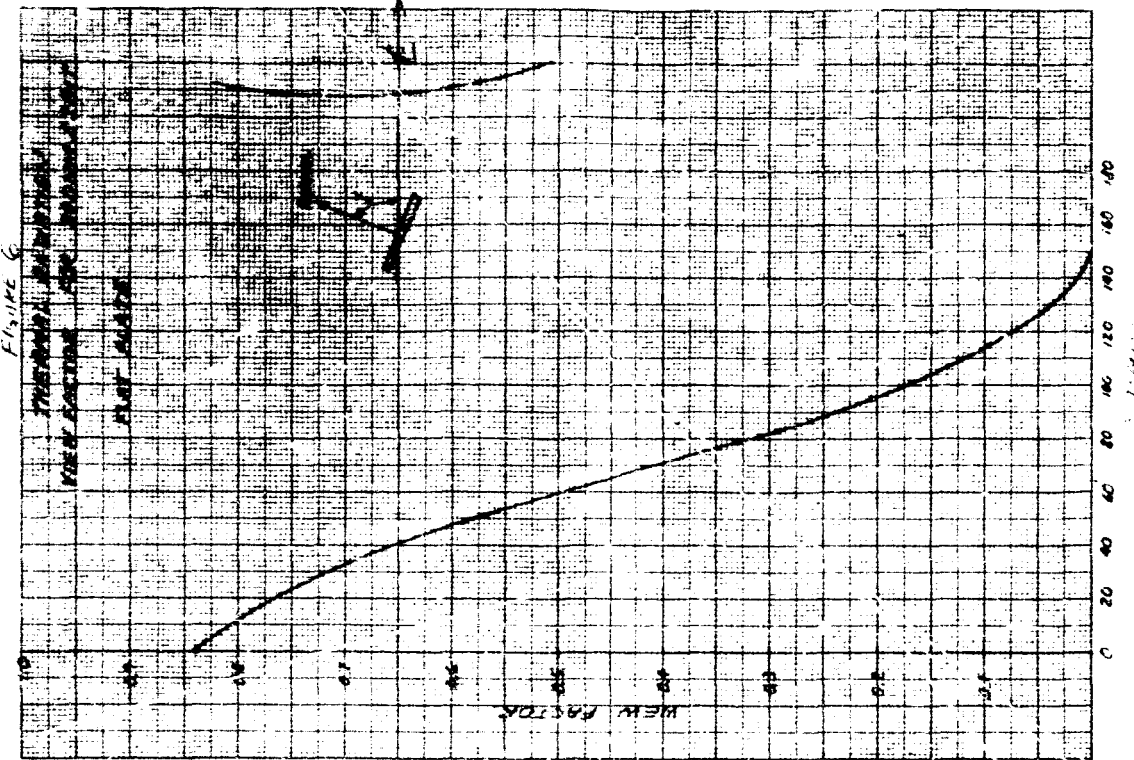


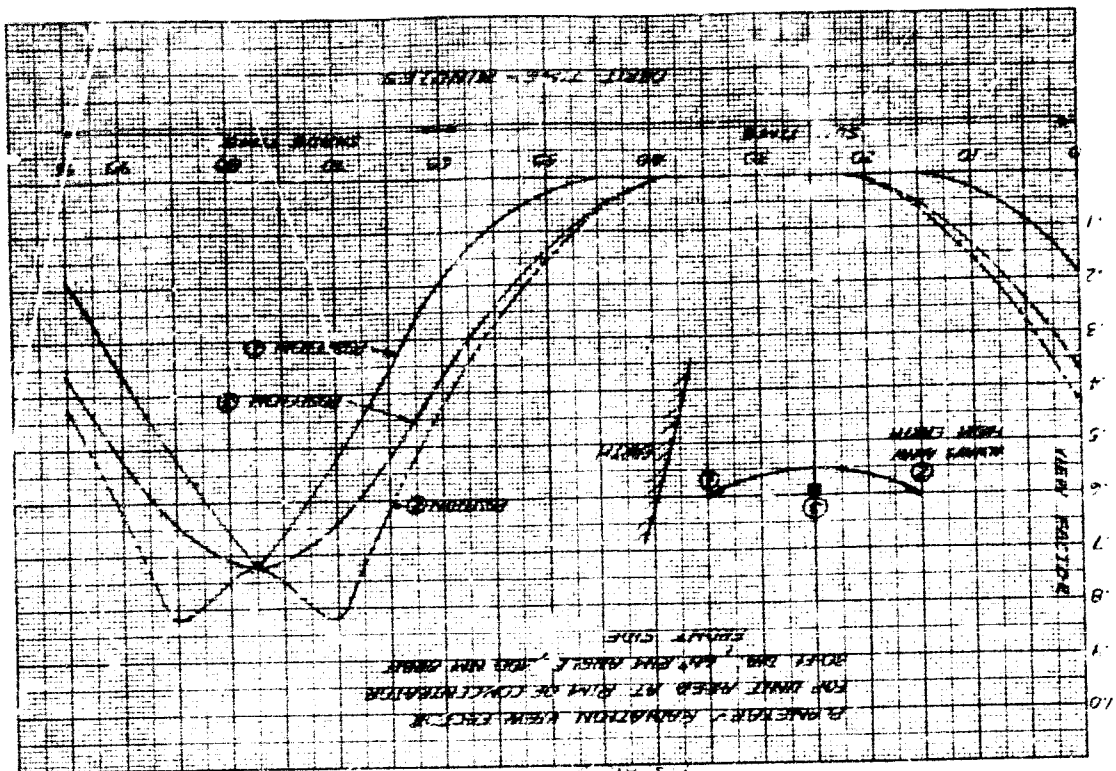
Figure 5

30% Max. O.D.
Surface error std. dev. = .10
Gandy radiation at 1000°

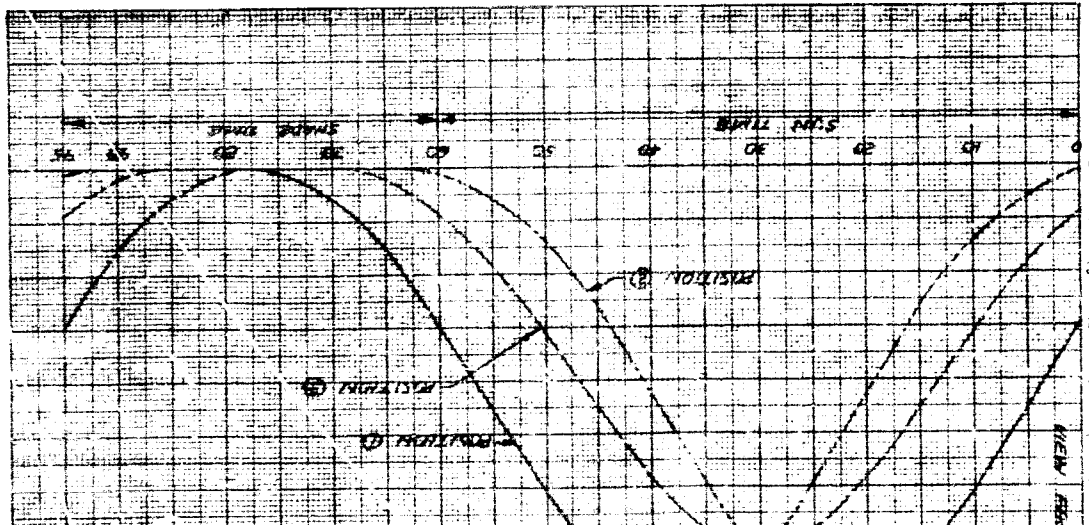




11-956 10-15 TO TAKE D. H. MURKIN



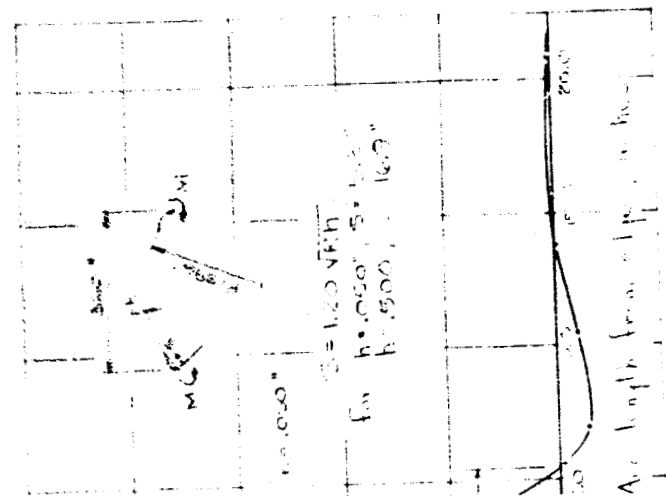
11-662 12-1310 13-1411 3-4



26

25

FIGURE 11



Relationship between Average Edge Length
for Edge Moment

FIGURE 12

